

Virtual tactile texture using electrostatic friction display for natural materials: The role of low and high frequency textural stimuli

Kazuya Otake¹, Shogo Okamoto^{1,2}, Yasuhiro Akiyama¹ and Yoji Yamada¹

1. Nagoya University, Aichi, Japan

2. Tokyo Metropolitan University, Tokyo, Japan

Abstract—As touchscreens have become a standard feature in mobile devices, technologies for presenting tactile texture feedback on the panel have been attracting attention. We tested a new method for presenting natural materials using an electrostatic tactile texture display. In this method, the frictional forces are decomposed into low- and high-frequency components. The low-frequency component was modeled based on Coulomb's friction law, such that the friction force was reactive to the finger's normal force. The high-frequency component was modeled using an auto-regressive model to retain its features of frequency spectra. Four natural material types, representing leather, cork, denim, and drawing paper, were presented to six assessors using this method. In a condition where only the low-frequency friction force components were rendered, the materials were correctly recognized at 70%. In contrast, when the high-frequency components were superposed, this rate increased to 80%, although the difference was not statistically significant. Our approach to combine a physical friction model and frequency spectrum for low- and high-frequency components, respectively, allows people to recognize virtual natural materials rendered on touch panels.

Index Terms—Tactile texture display, Electrostatic friction stimuli, Auto-regressive model, Natural materials

I. INTRODUCTION

As touch panels have become more prevalent as computer user interfaces, tactile feedback technologies for touch panels have been intensively studied [1]. One tactile display technology suitable for touchscreens is the friction-variable type. It presents tactile stimuli by manipulating the surface friction generated when tracing the panel with a finger. The electrostatic friction display is a type of friction-variable display; various studies have been conducted using this display type. For example, the roughness intensity perceived by humans on electrostatic friction displays has been investigated [2], [3], [4], [5].

The objective of our research is to develop a method to render natural material textures, comprising cloth and wood, on a tactile touch panel display. Previous studies of electrostatic friction displays have attempted to virtually present roughness textures with periodic surface asperities [2], [6], [7] and surface textures of natural materials [7], [8], [9], [10]. Whereas the virtual stimuli quality that simulated regular

roughness textures was relatively high, the method for presenting the surface texture of natural materials has not been well established. For example, some material textures can rarely be identified using existing methods. In contrast, vibrotactile display methods have been developed by numerous researchers to present virtual textures similar to those of natural materials by reproducing the frequency characteristics [11], [12], [13], [14], [15], [16], [17], [18].

We consider that simulating or representing the frequency response is not sufficient to generate virtual natural material textures, and realism can be improved by adopting a physically consistent model. However, it is difficult to apply the high-frequency component caused by the fine and irregular surface texture of natural materials. In this study, we used an electrostatic friction display to output virtual texture stimuli that simulate natural materials by combining two stimulus types: physical model-based and frequency-based. The shear frictional force, obtained by touching the material surface beforehand in our earlier study [19], was separated into low- and high-frequency components, and these were presented on our electrostatic friction display. The low-frequency component was represented based on Coulomb's friction law. The high-frequency component was approximated using an auto-regressive model. To evaluate these stimuli, we performed a texture discrimination task under two conditions: One in which only the physical model-based low-frequency component of the friction force was output, and the other in which a combination of low- and high-frequency texture components was output. Through this task, we investigated the extent to which the combined use of low- and high-frequency texture components contributed to the tactile texture transmitted from the panel to the fingertips. This study was approved by the Institutional Review Board of the School of Engineering, Nagoya University (#20-8).

II. APPARATUS: TACTILE TEXTURE DISPLAY USING ELECTROSTATIC FRICTION STIMULI

An electrostatic friction display changes the friction force by controlling the electrostatic attractive force generated by

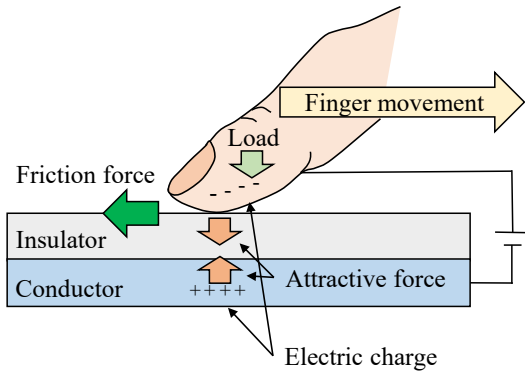


Fig. 1. Principles of electrostatic friction stimuli. The friction force is changed by controlling the electrostatic attractive force generated by the application of a voltage between the fingertip and panel. The friction force promotes the fingertip deformation in the shear direction.

applying a voltage between the fingertip and the panel, as shown in Fig. 1. This frictional force varies with the applied voltage magnitude and promotes fingertip deformation in the shear direction. Therefore, electrostatic friction stimuli are effective in presenting textured surfaces where frictional forces are dominant [8]. An insulator exists between the fingertip and panel and the current does not flow through the skin. In comparison with the vibrotactile display, the electrostatic displays do not involve mechanically driven parts, resulting in implementation advantages.

For the experiments, we used a tactile texture display that presents electrostatic friction stimuli, as shown in Fig. 2. Electrostatic friction stimuli were presented by applying a voltage between the fingertip and an indium tin oxide (ITO) panel to which an 8- μm insulating film (Kimotect PA8X, KIMOTO Co., Ltd., Japan) was attached. Experimental participants experienced stimulation by touching the panel while holding a stainless-steel rod connected to ground. The applied voltage was amplitude-modulated according to the algorithm described below (carrier frequency: 20 kHz). The modulated voltage signal was amplified by a voltage amplifier (HJOPS-1B20, Matsusada Precision Inc., Japan, maximum output: ± 1 kV, response: 75 kHz).

Four triaxial force sensors (USLG25, Tec Gihan Co., Ltd., Japan) were placed under the ITO panel to measure the normal and shear forces in real time. The fingertip position was estimated from the ratio of the four sensor outputs in the normal direction. The voltage amplifier and force sensors were connected to a DAQ board (PEX-361216, Interface Corporation, Japan). The sampling frequency for the force sensors was 125 Hz, and the control frequency for the friction display was 20 kHz.

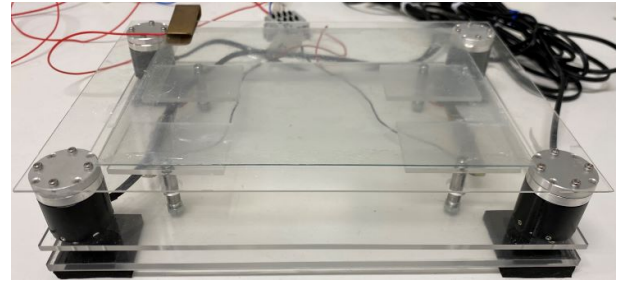


Fig. 2. Tactile texture display used in the experiments. Electrostatic friction stimuli were output from the ITO panel covered with an insulating film. Triaxis force sensors placed at the four corners measure the load on the finger and estimate its panel position.



Fig. 3. Four types of natural materials used in this experiment: leather, cork, denim, and drawing paper.

III. FRICTION MODELING FOR NATURAL MATERIAL TEXTURES

A. Four natural material types presented as virtual stimuli

We analyzed the friction force acquired in [19], where a variety of natural textures were scanned using a fingertip. The force data were resampled at 2 kHz. We selected four materials that are often touched in daily life: leather, cork, denim, and drawing paper, as shown in Fig. 3. If these natural materials are directly touched by bare fingers, they can be distinguished nearly 100%.

B. Division of friction into low- and high-frequency components

The frictional force generated when tracing surfaces with a finger ($f_s(t)$) is represented by,

$$f_s(t) = \mu_0 f_n(t) + \mu_t f_n(t), \quad (1)$$

by dividing it into a low-frequency component and a high-frequency texture component. μ_0 is the fixed friction coefficient of the material surface, $f_n(t)$ is the normal force or load on the finger, and μ_t is the high-frequency friction coefficient component above 2.5 Hz. The reason for setting 2.5 Hz as the threshold is that human finger movements are at most a few Hz [20], [21]. A Butterworth filter was used to separate the frictional forces by frequency. As an example,

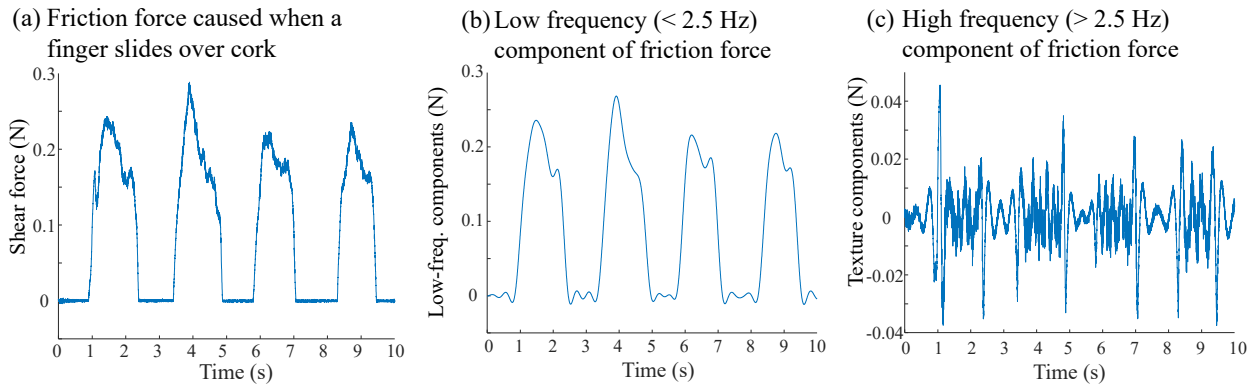


Fig. 4. Friction force data when the cork was traced. (a) Friction force caused when a finger slides over cork. (b) Low-frequency (< 2.5 Hz) friction force component. (c) High-frequency (> 2.5 Hz) friction force component.

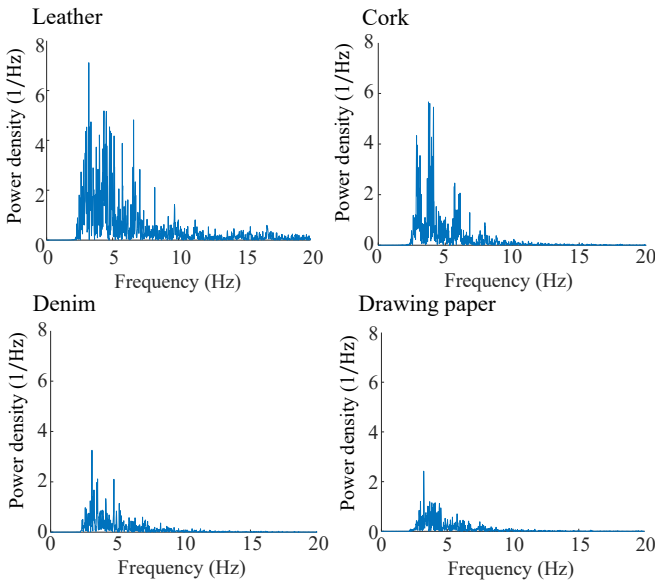


Fig. 5. Frequency response analysis of high-frequency shear force components using an auto-regressive model for each of the four natural materials. In the frequency range above 20 Hz, there is no significant difference between the materials; therefore, frequency responses within 0–20 Hz are indicated.

Fig. 4 shows the frictional force before and after separation when a cork is traced. (a) shows the original friction force ($f_s(t)$) when the cork is touched. (b) represents the low-frequency component below 2.5 Hz, and (c) represents the high-frequency component above 2.5 Hz.

The friction coefficient (μ_0) was determined by dividing the average shear force by the average normal force over 5 s measured when the material was touched. Table I lists the friction coefficients for each of the four natural materials. The material with the highest friction coefficient is leather ($\mu_0 = 0.51$), and the material with the lowest friction coefficient is drawing paper ($\mu_0 = 0.29$).

The high-frequency friction coefficient component was de-

termined by dividing the high-frequency friction force by the average normal force over 5 s. Fig. 5 shows the frequency characteristics of the high-frequency friction coefficient component. In the frequency range above 20 Hz, there was no significant difference between the materials. Therefore, only the frequency characteristics within 0–20 Hz are shown. However, it should be noted that the model contains additional high-frequency components.

C. Auto-regressive model for high-frequency components

This section describes the implementation procedure of the auto-regressive model for the texture components. First, we extracted only the moments when the fingers were clearly in contact with the material in the original force. Specifically, only the contact force at the moment when the normal force $f_n(t) > 0.05$ N and shear force $f_s(t) > 0.05$ N are valid was analyzed. Subsequently, we combined the time-series of the frictional force when the material was touched by five people who participated in the previous study [19] for each material and generated the contact force time-series of approximately 40–60 s. The auto-regressive model is given by:

$$x_k = \sum_{j=1}^p a_j x_{k-j} + v_k. \quad (2)$$

The model predicts the current value x_k from past values. This expresses the value of x_k by adding past p values. v_k represents the white noise. To determine the order p of the auto-regressive model, we used the Akaike information criterion (AIC):

$$\text{AIC} = -2L + 2p. \quad (3)$$

The AIC is expressed in two terms: the maximum log-likelihood L and the model p order. The larger the maximum log-likelihood, the smaller the AIC, and the easier it is to adopt as a model. Conversely, the second term, which grows in proportion to the model order, is added. Hence, models with large orders are less likely to be adopted. The p with the minimum AIC for each material is listed in Table II.

TABLE I
COEFFICIENT OF KINETIC FRICTION FOR EACH MATERIAL.

| Leather | Cork | Denim | Drawing paper |
|---------|------|-------|---------------|
| 0.51 | 0.45 | 0.38 | 0.29 |

TABLE II
ORDER p OF THE AUTO-REGRESSIVE MODEL FOR EACH MATERIAL.

| Leather | Cork | Denim | Drawing paper |
|---------|------|-------|---------------|
| 37 | 29 | 19 | 32 |

IV. EXPERIMENT: DISCRIMINATION OF VIRTUAL TEXTURES

For the four materials shown in Fig. 3, we prepared two conditions: One in which only Coulomb friction (low frequency) was output, and the other in which Coulomb and high-frequency friction components were simultaneously output. The accuracy of natural material discrimination under these two conditions was compared. To evaluate the realism of virtual textures, it is desirable to investigate both the subjective and behavioral performances; however, in the present study, we only investigated the behavioral ones. Further, we did not present only the high-frequency components. In order to do this, the tactile display needs to be able to decrease the coefficient of friction of the panel; however, the panel can only increase the coefficient.

A. Three-alternative-forced-choice task

We applied the forced n -choice task technique [22], [23], [24], [25] to each stimulus condition ($n = 3$). Two of the four types of virtual texture were randomly selected. One was presented twice, and the other was presented once. The participant answered which of the three virtual textures was different from the others. There were six combinations of two virtual textures among the four types of materials, and each combination was tested four times, resulting in 24 trials per participant in each stimulus condition. There was no time limit for the participants to touch the virtual textures. The participants washed their hands before the experiment. During the experiment, the fingertip surfaces were lubricated with talc to reduce the friction effect caused by finger moisture. During the trial, participants wore headphones and listened to pink noise.

B. Participants

Six university students (men in their 20s) participated in the experiment. All participants were unaware of the purpose of the experiment.

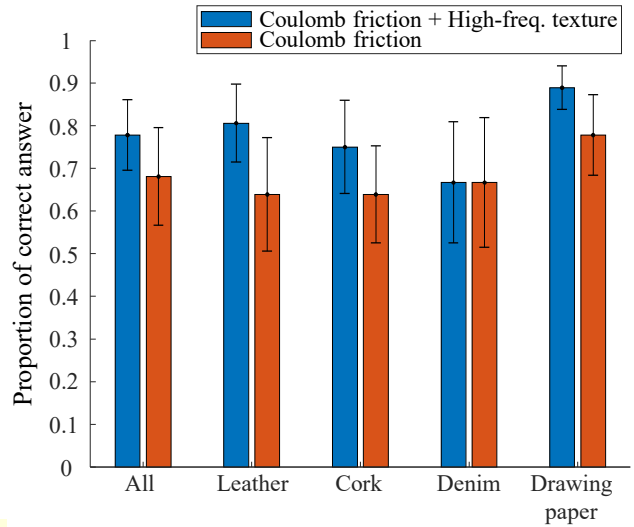


Fig. 6. Means and standard errors of correct answer proportions.

C. Electrostatic friction stimuli for virtual material stimuli

The relationship between the frictional force $f_s(t)$ and the applied voltage $V_e(t)$ is determined by the law of electrostatic force and Coulomb friction as,

$$f_s(t) = \mu\{f_n(t) + kV_e(t)^2\}, \quad (4)$$

where μ and k are the friction coefficient and constant related to the electrostatic force of the panel, respectively. Hence, to present the tangential force generated when tracing the panel with a finger, the applied voltage $V_e(t)$ is,

$$V_e(t) = \pm\alpha\sqrt{\mu_0 f_n(t) + \beta\mu_t f_n(t)}, \quad (5)$$

where α represents the gain to adjust the stimulus to the recognizable intensity for each participant. β is the gain that amplifies the high-frequency component features. The applied positive and negative voltages were switched by amplitude modulation at 20 kHz to alleviate the difficulty in feeling the stimulus owing to residual electric charges [26]. The virtual texture intensity α was adjusted by the participant before the three-alternative-forced-choice task such that s/he could recognize the frictional stimuli. The high-frequency component intensity, β , was adjusted in advance by the authors to the intensity where the difference among the four material types was most perceptible ($\beta = 1.8$).

V. RESULTS

Fig. 6 and Table III show the results of the three-alternative-forced-choice task. In Table III, (a) indicates Coulomb friction plus high-frequency texture condition and (b) indicates Coulomb friction only condition. The proportion of correct answers was calculated by dividing the total number of correct answers by the total number of trials. When a participant could select one different virtual stimulus among the three in a trial, the answer was categorized as correct. The error bars are the

TABLE III

MEANS AND STANDARD ERRORS OF ANSWER PROPORTIONS. (A) INDICATES COULOMB FRICTION PLUS HIGH-FREQUENCY TEXTURE CONDITION. (B) INDICATES COULOMB FRICTION ONLY CONDITION.

(a)

| | Actual natural materials | | | |
|---------------|--------------------------|-----------------|-----------------|-----------------|
| | Leather | Cork | Denim | Drawing paper |
| Leather | 0.81 ± 0.15 | 0.13 ± 0.04 | 0.03 ± 0.01 | 0.01 ± 0.01 |
| Cork | | 0.75 ± 0.16 | 0.14 ± 0.07 | 0.01 ± 0.01 |
| Denim | | | 0.67 ± 0.18 | 0.13 ± 0.05 |
| Drawing paper | | | | 0.89 ± 0.15 |

(b)

| | Actual natural materials | | | |
|---------------|--------------------------|-----------------|-----------------|-----------------|
| | Leather | Cork | Denim | Drawing paper |
| Leather | 0.64 ± 0.17 | 0.17 ± 0.04 | 0.08 ± 0.03 | 0.04 ± 0.03 |
| Cork | | 0.64 ± 0.15 | 0.14 ± 0.06 | 0.11 ± 0.05 |
| Denim | | | 0.67 ± 0.18 | 0.10 ± 0.05 |
| Drawing paper | | | | 0.78 ± 0.15 |

standard errors among the participants. A t -test was applied between the two stimulus conditions.

When all four materials were grouped together, the proportion of correct answers when both Coulomb friction and high-frequency texture components were output was 0.78 ± 0.08 , and when only the Coulomb friction component was output, the proportion was 0.68 ± 0.11 . There was no significant difference between the two stimulus conditions ($t = 0.63, p = 0.27$).

In the case of leather, the proportion of correct answers when both Coulomb friction and high-frequency texture components were output was 0.81 ± 0.09 , and when only the Coulomb friction component was output, the proportion was 0.64 ± 0.13 . There was no significant difference between the two stimulus conditions ($t = 0.94, p = 0.18$). As in Table III, leather was frequently confused with cork.

In the case of cork, the proportion of correct answers when both Coulomb friction and high-frequency texture components were output was 0.75 ± 0.11 , and when only the Coulomb friction component was output, the proportion was 0.64 ± 0.11 . There was no significant difference between the two stimulus conditions ($t = 0.64, p = 0.27$). As in Table III, cork tended to be misrecognized as leather and denim in Coulomb friction plus high-frequency texture condition.

In the case of denim, the proportion of correct answers when both Coulomb friction and high-frequency texture components were output was 0.67 ± 0.14 , and when only the Coulomb friction component was output, the proportion was 0.67 ± 0.15 . There was no difference in the percentage of correct responses between the two stimulus conditions ($t = 0, p = 0.5$). Denim was confused with cork and drawing paper in the Coulomb friction plus high frequency texture condition. Further, denim tended to be incorrectly answered as cork in the Coulomb

friction condition, as in Table III.

In the case of drawing paper, the proportion of correct answers when both Coulomb friction and high-frequency texture components were output was 0.89 ± 0.05 , and when only the Coulomb friction component was output, the proportion was 0.78 ± 0.09 . There was no significant difference between the two stimulus conditions ($t = 0.95, p = 0.18$). Drawing paper was frequently misclassified to be denim, as in Table III.

VI. DISCUSSION

We expected that the discrimination accuracy of virtual textures presented with electrostatic friction stimuli would be improved by combining the low-frequency component based on the physical model and the high-frequency component generated by the auto-regressive model, rather than only the low-frequency component. Overall, the former method improved the material discrimination accuracy, but the increase was not statistically significant. The primary reason for this was that the number of participants in the experiment was small. Contrary to our expectations, the participants were able to discriminate materials to some extent only by the low-frequency component of friction. Therefore, it is considered that the addition of the texture component did not significantly change the proportion of correct answers.

The combination of low- and high-frequency texture components increased the amount of information conveyed to the fingertips. Therefore there were more useful features for the participants to distinguish the materials. In addition to the low-frequency friction stimulus based on the physical model, the high-frequency friction stimulus based on the auto-regressive model may have made it easier to discriminate virtual textures.

In this experiment, Coulomb's law of friction was used as the physical model. However, it does not fully correspond to actual friction phenomena because it is a very simple model. A more advanced physical model based on skin contact mechanics must be developed in the future. For example, a model in which the coefficient of friction varies with the velocity and finger load [27] can be considered.

VII. CONCLUSION

We developed a method for presenting the tactile texture of natural materials through an electrostatic friction display and experimentally investigated its effectiveness. We investigated whether the combination of low-frequency friction components based on Coulomb's law and high-frequency texture components could enhance the discrimination of the four virtual material types. Although the results could not be clearly stated in statistical terms, the combination of the two resulted in correct discrimination with a probability of approximately 80%. Adopting a more physically valid model than that used in the current study may improve the quality of the stimuli.

ACKNOWLEDGMENTS

This study was in part supported by MEXT KAKENHI (#20H04263).

REFERENCES

- [1] C. Basdogan, F. Giraud, V. Levesque, and S. Choi, "A review of surface haptics: Enabling tactile effects on touch surfaces," *IEEE Transactions on Haptics*, vol. 13, no. 3, pp. 450–470, 2020.
- [2] A. Isleyen, Y. Vardar, and C. Basdogan, "Tactile roughness perception of virtual gratings by electrovibration," *IEEE Transactions on Haptics*, vol. 13, no. 3, pp. 562–570, 2020.
- [3] H. Tomita, S. Saga, H. Kajimoto, S. Vasilache, and S. Takahashi, "A study of tactile sensation and magnitude on electrostatic tactile display," in *Proceedings of IEEE Haptics Symposium*, 2018, pp. 158–162.
- [4] O. Bau, I. Poupyrev, A. Israr, and C. Harrison, "Teslatouch: electrovibration for touch surfaces," in *Proceedings of Annual ACM Symposium on User Interface Software and Technology*, New York, 2010, pp. 283–292.
- [5] D. Wijekoon, M. Cecchinato, E. Hoggan, and J. Linjama, "Electrostatic modulated friction as tactile feedback: intensity perception," in *Haptics: Perception, Devices, Mobility, and Communication*, 2012, pp. 613–624.
- [6] K. Ito, S. Okamoto, Y. Yamada, and H. Kajimoto, "Tactile texture display with vibrotactile and electrostatic friction stimuli mixed at appropriate ratio presents better roughness textures," *ACM Transactions on Applied Perception*, vol. 16, no. 4, 2019.
- [7] K. Otake, H. Hasegawa, S. Okamoto, and Y. Yamada, "Virtual roughness textures via a surface tactile texture display using vibrotactile and electrostatic friction stimuli: Improved realism," in *Proceedings of 13th International Conference on Human System Interaction*, 2020, pp. 147–152.
- [8] T. Fielder and Y. Vardar, "A novel texture rendering approach for electrostatic displays," in *Proceedings of International Workshop on Haptic and Audio Interaction Design*, no. hal-02011782v3, 2019.
- [9] J. Jiao, Y. Zhang, D. Wang, Y. Visell, D. Cao, X. Guo, and X. Sun, "Data-driven rendering of fabric textures on electrostatic tactile displays," in *Proceeding of IEEE Haptics Symposium*, 2018, pp. 169–174.
- [10] G. Ilkhani, M. Aziziaghdam, and E. Samur, "Data-driven texture rendering on an electrostatic tactile display," *International Journal of Human-Computer Interaction*, vol. 33, no. 9, pp. 756–770, 2017.
- [11] H. Culbertson, J. Unwin, and K. J. Kuchenbecker, "Modeling and rendering realistic textures from unconstrained tool-surface interactions," *IEEE Transactions on Haptics*, vol. 7, no. 3, pp. 381–393, 2014.
- [12] R. Hassen and E. Steinbach, "Vibrotactile signal compression based on sparse linear prediction and human tactile sensitivity function," in *Proceedings of IEEE World Haptics Conference*, 2019, pp. 301–306.
- [13] M. Wiertelwski, J. Lozada, and V. Hayward, "The spatial spectrum of tangential skin displacement can encode tactual texture," *IEEE Transactions on Robotics*, vol. 27, no. 3, pp. 461–472, 2011.
- [14] B. Camillieri, M.-A. Bueno, M. Fabre, B. Juan, B. Lemaire-Semail, and L. Mouchnino, "From finger friction and induced vibrations to brain activation: Tactile comparison between real and virtual textile fabrics," *Tribology International*, vol. 126, pp. 283–296, 2018.
- [15] J. M. Romano and K. J. Kuchenbecker, "Creating realistic virtual textures from contact acceleration data," *IEEE Transactions on Haptics*, vol. 5, no. 2, pp. 109–119, 2012.
- [16] Y. Matsuura, S. Okamoto, S. Asano, H. Nagano, and Y. Yamada, "A method for altering vibrotactile textures based on specified materials," in *Proceeding of IEEE International Symposium on Robot and Human Interactive Communication*, 2012, pp. 995–1000.
- [17] S. Asano, S. Okamoto, Y. Matsuura, and Y. Yamada, "Toward quality texture display: vibrotactile stimuli to modify material roughness sensations," *Advanced Robotics*, vol. 28, no. 16, pp. 1079–1089, 2014.
- [18] S. Okamoto and Y. Yamada, "Perceptual properties of vibrotactile material texture: Effects of amplitude changes and stimuli beneath detection thresholds," in *2010 IEEE/SICE International Symposium on System Integration*, 2010, pp. 384–389.
- [19] H. Hasegawa, S. Okamoto, and Y. Yamada, "Phase difference between normal and shear forces during tactile exploration represents textural features," *IEEE Transactions on Haptics*, vol. 13, no. 1, pp. 11–17, 2020.
- [20] H.-J. Freund, "Time control of hand movements," in *The Oculomotor and Skeletalmotor Systems: Differences and Similarities*, ser. Progress in Brain Research, 1986, vol. 64, pp. 287–294.
- [21] E. Kunesch, F. Binkofski, and H.-J. Freund, "Invariant temporal characteristics of manipulative hand movements," *Experimental Brain Research*, vol. 78, pp. 539–546, 1989.
- [22] R. Fagiani, F. Massi, E. Chatelet, Y. Berthier, and A. Akay, "Tactile perception by friction induced vibrations," *Tribology International*, vol. 44, no. 10, pp. 1100–1110, 2011.
- [23] J. T. Townsend and D. E. Landon, "An experimental and theoretical investigation of the constant-ratio rule and other models of visual letter confusion," *Journal of Mathematical Psychology*, vol. 25, no. 2, pp. 119–162, 1982.
- [24] S. Okamoto, "VR-MDS: Multidimensional scaling for classification tasks of virtual and real stimuli," *Attention Perception & Psychophysics*, vol. 76, no. 3, pp. 877–893, 2014.
- [25] F. R. Clarke, "Constant-ratio rule for confusion matrices in speech communication," *Journal of the Acoustical Society of America*, vol. 29, no. 6, pp. 715–720, 1957.
- [26] T. Nakamura and A. Yamamoto, "Modeling and control of electroadhesion force in dc voltage," *Robomech Journal*, vol. 4, no. 18, 2017.
- [27] K. Inoue, S. Okamoto, Y. Akiyama, and Y. Yamada, "Effect of material hardness on friction between a bare finger and dry and lubricated artificial skin," *IEEE Transactions on Haptics*, vol. 13, no. 1, pp. 123–129, 2020.